Tumor cell-selective regulation of NOXA by c-MYC in response to proteasome inhibition

Mikhail A. Nikiforov*†, MaryBeth Riblett*†, Wen-Hua Tang*†, Vladimir Gratchouck*†, Dazhong Zhuang*†, Yolanda Fernandez*†‡, Monique Verhaegen*†, Sooryanarayana Varambally†§, Arul M. Chinnaiyan†§, Andrzej J. Jakubowiak§¶, and Maria S. Soengas*†‖

Departments of *Dermatology and ¶Internal Medicine, †Comprehensive Cancer Center, and §Michigan Center for Translational Pathology, University of Michigan, Ann Arbor, MI 48109

Edited by Tak Wah Mak, University of Toronto, Toronto, ON, Canada, and approved October 3, 2007 (received for review September 5, 2007)

The proteasome controls a plethora of survival factors in all mammalian cells analyzed to date. Therefore, it is puzzling that proteasome inhibitors such as bortezomib can display a preferential toxicity toward malignant cells. In fact, proteasome inhibitors have the salient feature of promoting a dramatic induction of the proapoptotic protein NOXA in a tumor cell-restricted manner. However, the molecular determinants that control this specific regulation of NOXA are unknown. Here, we show that the induction of NOXA by bortezomib is directly dependent on the oncogene c-MYC. This requirement for c-MYC was found in a variety of tumor cell types, in marked contrast with dispensable roles of p53, HIF-1α, and E2F-1 (classical proteasomal targets that can regulate *NOXA* mRNA under stress). Conserved MYC-binding sites identified at the *NOXA* promoter were validated by ChIP and reporter assays. Down-regulation of the endogenous levels of c-MYC abrogated the induction of NOXA in proteasome-defective tumor cells. Conversely, forced expression of c-MYC enabled normal cells to accumulate NOXA and subsequently activate cell death programs in response to proteasome blockage. c-MYC is itself a proteasomal target whose levels or function are invariably up-regulated during tumor progression. Our data provide an unexpected function of c-MYC in the control of the apoptotic machinery, and reveal a long sought-after oncogenic event conferring sensitivity to proteasome inhibition.

drug selectivity | melanoma | oncogenes | apoptosis | Bcl-2 family

Proteasome inhibitors such as bortezomib are raising high expectation as anticancer agents, based on their ability to kill a broad spectrum of tumor cell types (1, 2). The potential efficacy of these compounds is perhaps not surprising, considering the well established role of the 26S proteasome in the control of cell cycle progression, apoptosis, and response to oncogenic stress (3). However, the fact that proteasome inactivation can display tolerable secondary toxicities is counterintuitive, because the half-life of nearly 80% of cellular proteins is under proteasomal control also in normal cells (2, 3). The molecular mechanisms underlying the tumor cell selectivity of proteasome inhibitors remain largely unknown (1).

By using melanoma as an example of a highly chemoresistant tumor type, we and others have previously identified the protein NOXA as the first proapoptotic factor induced by bortezomib preferentially in cancer cells (4, 5). For example, bortezomib promoted a 20- to 60-fold induction of NOXA in a large panel of melanoma cells, whereas levels in normal melanocytes remained barely detectable (4–7). Similar results were obtained with other proteasome inhibitors and in cells from breast cancer, small cell lung cancer, T cell leukemia, multiple myeloma, mantle-cell lymphoma, and squamous cell carcinoma (4, 5, 8–10). This tumor cell-restricted induction of NOXA could not be recapitulated by standard chemotherapeutic agents such as doxorubicin, etoposide, or cisplatin, emphasizing a unique impact of bortezomib on the apoptotic machinery of tumor cells (4, 5).

Human *NOXA* was initially identified as a phorbol ester-responsive gene (11). However, the role of this protein in apoptosis became apparent when the murine homologue was identified as a p53 transcriptional target involved in the response to UV and a variety of DNA-damaging drugs (12–14). The transcriptional factors HIF-1α and E2F-1 can also transactivate *NOXA* mRNA, suggesting a broad function in the response to cellular stress (15, 16). In terms of functional domains, human NOXA contains one BH3 (Bcl-2 homology 3) domain, which has a high affinity for the antiapoptotic factor Mcl-1 (17–19). MCL-1 is a ubiquitin target, and thus, it is up-regulated when the proteasome is inhibited (20). NOXA is essential to counteract this high expression of MCL-1 and allow for the activation of the apoptotic machinery in response to bortezomib (7).

The *NOXA* gene is not mutated or amplified during tumor development (21). Therefore, a key question is why NOXA protein levels are induced by bortezomib preferentially in cancer cells but not in their normal counterparts. We and others have shown that the proteasome modulates not only the half-life of NOXA protein but also its mRNA levels (4, 5). In this study, we address mechanisms controlling NOXA mRNA transcription to identify molecular determinants underlying the tumor cell selectivity of proteasome inhibitors. Unexpectedly, neither p53, HIF-1α, nor E2F-1 were found to be essential for the proteasomal regulation of NOXA. Instead, we identify the oncogene c-MYC as a direct modulator of *NOXA* mRNA, and essential for the tumor cell-selective regulation of NOXA by the proteasome. This study unveils an unexpected mechanism of regulation of the apoptotic machinery by c-MYC and underscores a strategy to exploit the altered genetic background of tumor cells for a specific induction of cell death.

Results

The Induction of NOXA by Bortezomib Is Dependent on New mRNA Synthesis. Bortezomib can induce NOXA protein and mRNA levels (4, 5). However, the relative contribution of these two levels of regulation to the ultimate expression of NOXA is unclear (i.e., transcription *de novo* may be dispensable if a preexisting pool of NOXA protein is stabilized). To address this question, we first focused on the melanoma cell lines SK-Mel-19 and SK-Mel-103, as two representative examples of tumor cells that are highly responsive to bortezomib [see supporting information (SI) Fig. 6*A*].

Author contributions: M.A.N. and M.S.S. designed research; M.A.N., M.R., W.-H.T., V.G., D.Z., Y.F., M.V., and M.S.S. performed research; M.A.N., D.Z., S.V., A.M.C., and A.J.J. contributed new reagents/analytic tools; M.A.N. and M.S.S. analyzed data; and M.S.S. wrote the paper.

The authors declare no conflict of interest.

This article is a PNAS Direct Submission.

‡Present address: Merck KGaA, Bioresearch Laboratory, Parc Científic de Barcelona, 08028 Barcelona, Spain.

‖To whom correspondence should be addressed at: University of Michigan Comprehensive Cancer Center (4217 CCGC), 1500 East Medical Center Drive, Ann Arbor, MI 48109. E-mail: soengas@umich.edu.

This article contains supporting information online at www.pnas.org/cgi/content/full/0708380104/DC1.

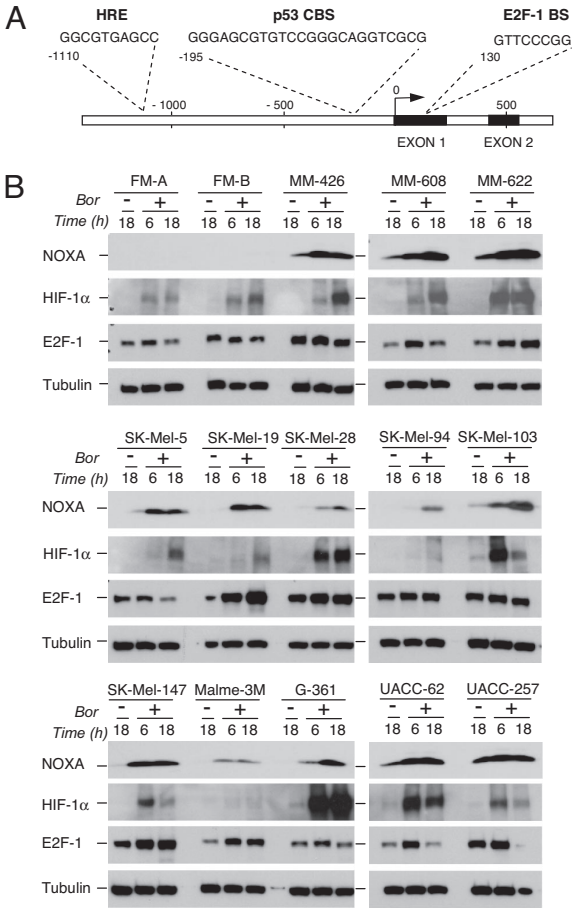

Fig. 1. Lack of correlation between NOXA protein levels and HIF-1α or E2F-1. (*A*) Human *NOXA* promoter showing the location and sequence of a HRE and binding sites for p53 (p53 CBS) and E2F-1 (E2F-1 BS). (*B*) Expression of NOXA, HIF-1α, and E2F-1 in total cell extracts prepared from two independent populations of normal human foreskin melanocytes (FM) and the indicated melanoma cell lines, incubated in the absence (−) or presence (+) of 50 nM bortezomib.

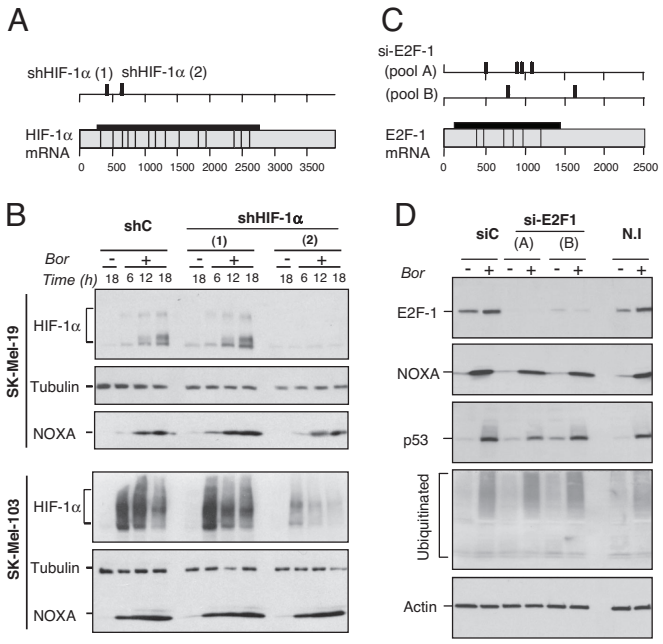

Fig. 2. No functional interdependence of NOXA and HIF-1α or E2F-1. (*A*) Schematic representation of the shRNAs to down-regulate HIF-1α by shRNA. Exons are indicated with gray boxes, and the coding region is indicated with a horizontal black bar. Numbers correspond to nucleotide positions from the transcriptional starting site. (*B*) Immunoblots corresponding to SK-Mel-19 or SK-Mel-103 infected with lentiviruses coding for control (shC) or HIF-1α short hairpins (sh HIF-1α) and treated with vehicle (−) or 50 nM bortezomib (+). shHIF1α (1) was found inactive and served as a control for unspecific events of lentiviral infection. (*C*) Pools of siRNAs used to inhibit E2F-1 expression and their complementarity sites depicted as in *A*. (*D*) Levels of E2F-1 and the indicated proteins in SK-Mel-103 transduced with control or E2F-1 siRNAs pools (A or B) and incubated in vehicle (−) or 25 nM bortezomib (−) for 10 h. N.I., noninfected cells.

Human melanocytes were also used as a control for normal cells in which bortezomib fails to promote the accumulation of NOXA, despite an efficient inactivation of the proteasome (SI Fig. 6*A*). By using this time course as a reference, cells were treated with bortezomib in the presence or absence of actinomycin D (Act D), a classical transcriptional inhibitor. As shown in SI Fig. 6*B*, low doses of Act D (not toxic for melanoma cells) were found to inhibit bortezomib-driven expression of NOXA by 90%. Therefore, these results emphasize a key role of *de novo NOXA* mRNA transcription in the response of cancer cells to bortezomib.

p53, HIF-1a, and E2F-1 Are Not Essential Modulators of Bortezomib-Driven NOXA Accumulation. The human *NOXA* promoter contains a p53 binding site and a hypoxia response element (HRE) at positions −195 and −1110, respectively, from the transcriptional starting site (ENSG00000141682) (Fig. 1*A*). The impact of E2F-1 on human NOXA has not been addressed, but the E2F-1 binding site GTTCCCGG at position −48 in the mouse *noxa* promoter (ENSMUSG00000024521) can be found at nucleotide +130 in the human *NOXA* sequence (Fig. 1*A*).

NOXA can be induced by bortezomib in a variety of tumor cell lines with defective p53 signaling (see SI Fig. 7*A*). Moreover, a variety of clinical studies indicate that bortezomib can block tumor growth in a p53-independent manner (2, 22). However, cooperative effects between p53 and bortezomib have been described in refs. 9 and 23. Therefore, it is conceivable that, although p53 is not strictly required for transcription of *NOXA* mRNA, it can still contribute as a cofactor to the accumulation of NOXA protein in bortezomib-treated cells. However, abrogation of p53 expression by short interfering RNAs (shRNAs) had no impact on the induction of NOXA and subsequent induction of cell death by bortezomib (SI Fig. 7 *B* and *C*).

Next, we analyzed the relative expression of HIF-1α and E2F-1 at different time points after bortezomib treatment of melanocytes and a panel of 13 melanoma cell lines (to account for intraspecimen variability). Surprisingly, no obvious correlation was found between NOXA and HIF-1α or E2F-1 across cell lines (Fig. 1*B*). Importantly, down-regulating the endogenous levels of HIF-1α with highly efficient shRNAs (Fig. 2 *A* and *B*) or increasing HIF-1α levels by placing cells in hypoxia (SI Fig. 8*A*, right image), failed to alter the induction of NOXA by bortezomib in melanoma cells. Hypoxia was also not sufficient to allow for NOXA accumulation in bortezomib-treated melanocytes (SI Fig. 8*A*, left image).

E2F-1 was also found to be dispensable for the induction of NOXA by bortezomib. Two independent pools of short interfering RNA duplexes targeting a total of six different sites in the *NOXA* mRNA (Fig. 2*C*) were unable significantly affect the up-regulation of NOXA by bortezomib in melanoma cells, although the proteasome was efficiently inhibited (Fig. 2*D*). Conversely, melanocytes could not be sensitized to bortezomib-driven NOXA induction, even on forced expression of E2F-1 (SI Fig. 8 *B* and *C*).

Consensus MYC-Binding Sites in *NOXA* Promoter. Computer-based analyses performed on sequences spanning 4 kb upstream and downstream of the *NOXA* transcriptional starting site rendered a

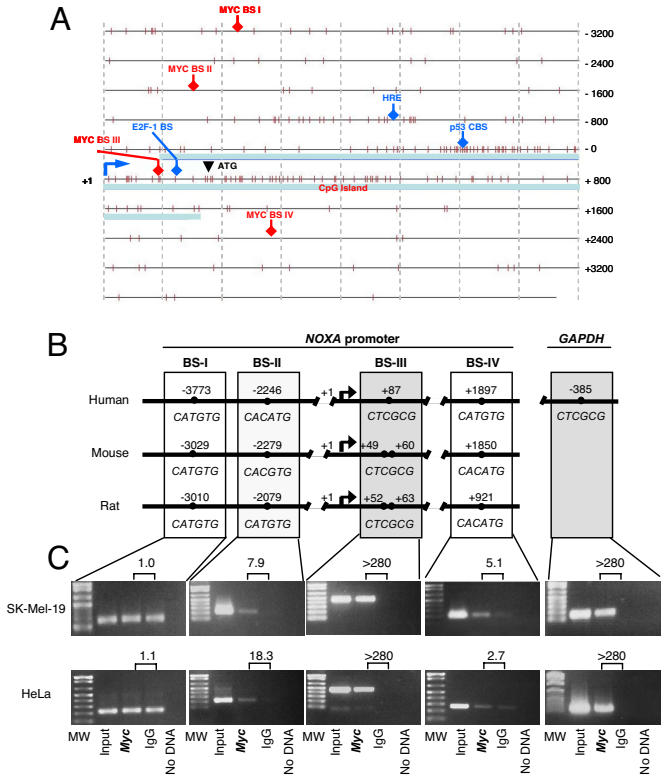

Fig. 3. Identification and validation of c-MYC binding sites at the *NOXA* promoter. (*A*) Genomic area flanking the *NOXA* transcriptional starting site (indicated as +1 position). Known binding sites for p53, hypoxia (HRE), and E2F-1 are shown in blue, and the newly identified putative MYC binding sites (BS I–IV) are shown in red. CpG dinucleotides are depicted with small vertical marks and the CpG island is indicated in light blue. (*B*) Promoters of human, mouse, and rat *NOXA*. The c-MYC binding site at the *GAPDH* promoter is shown as a comparison. (*C*) c-MYC binding to the NOXA promoter by ChIP. Parallel reactions included analyses of the c-MYC binding site in *GAPDH*. The specificity of binding of c-MYC to each putative site was estimated with respect to the IgG control as described in *Materials and Methods*.

large set of consensus binding sites for known transcriptional factors (data not shown). Therefore, additional restriction criteria were needed to narrow the list of candidates for subsequent functional analyses. Because NOXA, as other Bcl-2 proteins, is highly conserved in mammalian species, we hypothesized that the transcriptional control may also be shared. Therefore, comparative analyses were extended to mouse and rat *NOXA* sequences. In addition, we focused on factors controlled by the proteasome and deregulated during tumor progression. This approach led to the identification of the oncoprotein c-MYC as a putative transcriptional modulator of *NOXA* mRNA.

As depicted in Fig. 3*A*, four putative c-MYC binding sites (herein referred to BS I–IV), were found in the human *NOXA* promoter at positions −3773, −2246, +87, and +1897 (Fig. 3 *A* and *B*). The BS III (CTCGCG) was found to be particularly intriguing. First, it is conserved among the three species analyzed. Second, analysis of the surrounding sequences indicated that this site mapped within a CpG island (Fig. 3*A*), which is a frequent feature of c-MYC targets (24). And, finally, this noncanonical MYC-binding site was shown to be recognized by c-MYC, *in vitro* and *in vivo*, as a part of the promoter of the c-MYC target *GAPDH* (25, 26).

Endogenous c-MYC Interacts with NOXA Promoter *in Vivo*. Well characterized antibodies against c-MYC and IgG (the latter as negative control) were used to define the binding of c-MYC to the *NOXA* promoter by ChIP. By using SK-Mel-19 as a representative example of an aggressive melanoma line, a >280-fold higher enrichment of amplified DNA was detected with the c-MYC antibody (Fig. 3*C*). Of note, a similar effective binding was found for a well defined region of GAPDH promoter (26) containing the same MYC-binding site (Fig. 3 *B* and *C*). BS II and IV were bound less efficiently (i.e., the enrichment of precipitated material provided by the c-MYC antibody was 5.1- and 7.9-fold, respectively). No specific c-MYC binding was found at the more distant c-MYC BS I (Fig. 3*C*). A similar pattern of recognition of the c-MYC binding sites was found in HeLa (see Fig. 3*C*, lower images), indicating that the binding of c-MYC to the NOXA promoter is not exclusive of melanoma cells.

Bortezomib-Driven and c-MYC-Dependent Transactivation of the NOXA Promoter. In cancer cells, c-MYC is regulated in part by posttranscriptional mechanisms (27, 28). Therefore, we expected that the induction of NOXA by bortezomib would depend not on the basal levels of c-*MYC* mRNA, but on the ability of c-MYC to bind and recognize the *NOXA* promoter. In fact, c-*MYC* mRNA levels remained rather constant with treatment, whereas a 3- to 6-fold induction in the levels of c-MYC protein was observed in nearly all cell lines analyzed (Fig. 4*A* and SI Fig. 9*A*). Intriguingly, in seven of nine cases (SK-Mel-19, -28, -29, -103, -173, G-361, and UACC-62), NOXA mRNA and protein increased after progressive incubation with bortezomib, although there was not a strict linear correlation with c-MYC protein expression (see representative immunoblots in Fig. 4*A* and quantifications of immunoblots and RT-PCR analyses in SI Fig. 9 *A* and *B*). Therefore, bortezomib may control not only the expression, but the activity of c-MYC at the *NOXA* promoter.

To further characterize the impact of the proteasome at the NOXA promoter, additional ChIP assays were performed in the absence and presence of bortezomib. As shown in SI Fig. 10 *A* and *B*, bortezomib increased by 2- to 3-fold the amount of c-MYC at the MYC-BS III (either by stabilizing its binding or by enhancing its effective concentration). This effect of bortezomib was not found at BS I (where no specific binding of c-MYC was detected). Notably, a comparable enrichment of acetylated histone H3 was also determined at the MYC-BS III (SI Fig. 10 *A* and *B*), consistent with a transcriptional active site (29, 30), as described for other c-MYC targets (31). Mutagenizing the BS III, significantly abrogated the transcriptional activation by bortezomib at the *NOXA* promoter in luciferase-based reporter assays (SI Fig. 10*C*). Taken together, these results identify NOXA as a direct target of c-MYC.

Depletion of c-MYC by RNA Interference Abrogates the Tumor Cell-Selective Induction of NOXA by Bortezomib. The role of the endogenous levels of c-MYC on the regulation of NOXA by bortezomib was analyzed with a previously validated shRNA (32) that has minor effects on cell viability at least during 6 days after infection (Fig. 4*B*). By using this system, c-MYC levels were reduced by 80%. This inhibition of c-MYC abrogated the induction of NOXA by bortezomib without displaying unspecific effects on the proteolytic activity of the proteasome (Fig. 4*C*). For example, the proteasome targets p53 and MCL-1 were induced with similar kinetics in melanoma cells expressing c-MYC- or control-shRNA (Fig. 4*C*).

As we previously reported, bortezomib induces NOXA in a broad spectrum of tumor cell types. Therefore, we expected that the impact of c-MYC on the regulation of this protein would be tumor cell type independent. We showed that this was the case by using representative lines of melanoma (SK-Mel-19, -103, -147), breast cancer (MDA-MB-231), and cervical carcinoma (HeLa). In all these lines, c-MYC down-regulation caused a marked reduction (70–80%) in the amount of NOXA accumulated after bortezomib treatment (Fig. 4*D* and results not shown).

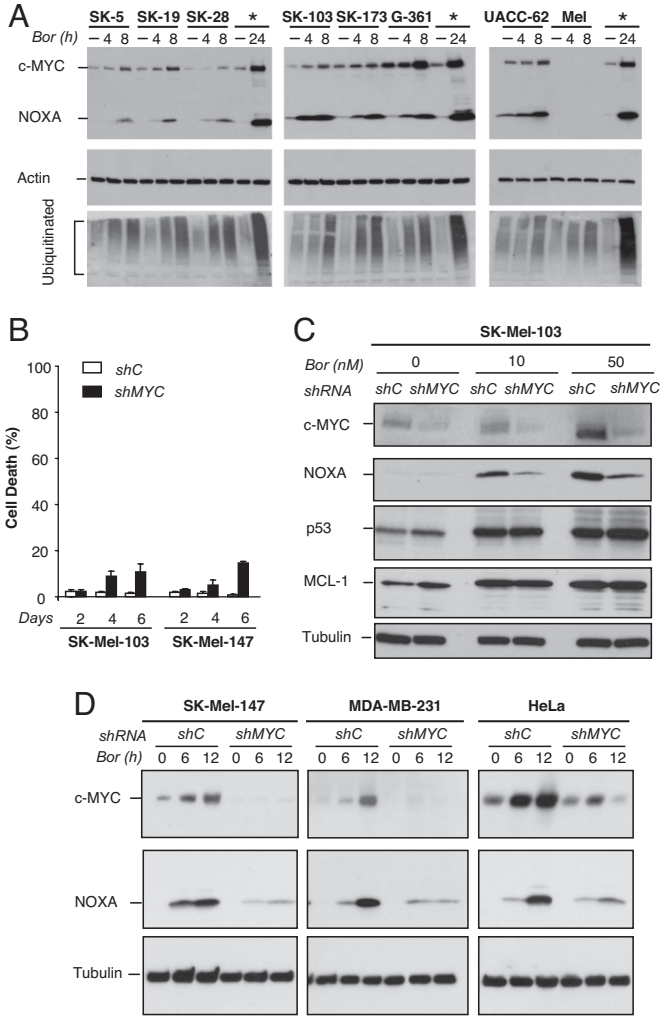

Fig. 4. Functional requirement of c-MYC for NOXA regulation. (*A*) Relative expression of c-MYC and NOXA visualized by immunoblotting in melanocytes (Mel) or a panel of melanoma cell lines treated with 25 nM bortezomib for the indicated time points. Asterisks correspond to the HCT116 colon carcinoma cell line, used here as internal control for comparable staining of independent blots (and as an example of cells from other tumor type). Actin and ubiquitinated proteins are shown as references for protein loading and proteasome inhibition by bortezomib, respectively. (*B*) Lack of toxicity of c-MYC shRNA. Cell death is shown as average of triplicates ± SE estimated by trypan blue exclusion at the indicated times (in days) after infection. (*C*) Down-regulation of c-MYC by shRNA and concomitant inhibition of the induction of NOXA by bortezomib. Cells were treated with the indicated doses of bortezomib for 6 h. p53 and Mcl-1 levels were tested to assess unspecific effects of the shRNAs on classical proteasome targets that can affect NOXA function. (*D*) Blockage of NOXA up-regulation by bortezomib (50 nM) on transduction of shC or shMYC in cells from melanoma (SK-Mel-147), breast cancer (MDA-MB-231), and cervical carcinoma (HeLa).

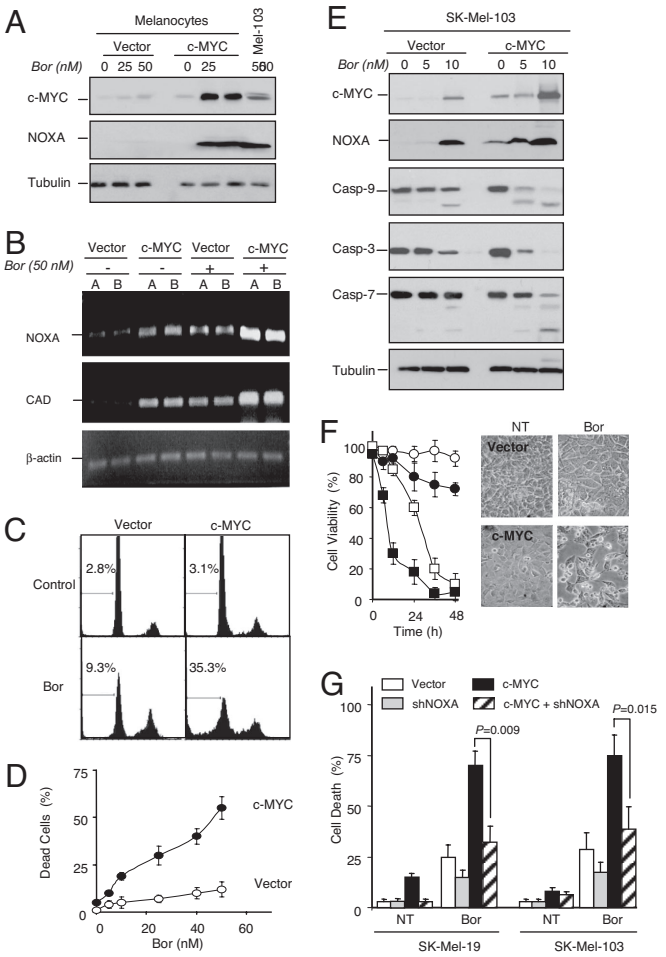

Fig. 5. Direct contribution of c-MYC to bortezomib/NOXA-driven cell death. (*A*) Lentivirus-mediated overexpression of c-MYC in normal melanocytes allows for NOXA induction after bortezomib treatment. SK-Mel-103 treated with bortezomib is shown as a positive reference. (*B*) Increased NOXA mRNA by c-MYC determined by RT-PCR. β-Actin and the classical c-MYC target CAD (carbamoyl-phosphate synthetase 2, aspartate transcarbamylase, and dihydroorotase) are shown as references. (*C*) Changes in DNA content induced by 50 nM bortezomib (12 h), visualized by propidium iodide staining and flow cytometry. The amount of cells with degraded DNA (sub-G_1 fraction) is indicated in percentages. (*D*) Increased bortezomib-mediated cell death of MYC-overexpressing melanocytes estimated by trypan blue exclusion and represented as the mean ± SE of three independent experiments. (*E–G*) Forced expression of c-MYC accelerates NOXA expression and caspase processing as determined by immunoblotting (*E*). (*F*) (*Left*) Measurement of cell viability by MTT assays of SK-Mel-19 expressing shC (white symbols) or shMYC (black symbols), and treated with vehicle control (circles) or with 10 nM bortezomib (squares). (*Right*) Representative microphotographs of cells untreated (NT) or treated with bortezomib. (*G*) Quantification of the sensitizing effect of c-MYC and the functional requirement of NOXA. The indicated melanoma cell lines were infected with control lentiviral vectors or vectors expressing NOXA shRNA. Cells were subsequently transduced with c-MYC and left untreated or treated with low doses of bortezomib (10 nM). Values correspond to the amount of dead cells collected 12 h after treatment (represented as means ± SD of three experiments). The *t* test was used to determine the statistical significance of NOXA down-regulation in the response to bortezomib of control and c-MYC-overexpressing cells.

c-MYC Sensitizes Normal Melanocytes to Bortezomib-Induced NOXA Activation. Next, melanocytes were transduced with exogenous levels of c-MYC to determine whether this transcription factor is sufficient to enhance *NOXA* mRNA in primary cells. To this end, fresh preparations of normal human skin melanocytes were infected with lentiviruses coding for human c-MYC, at multiplicities of infection that allow for the expression of c-MYC within four to eight times the basal levels in tumor cells (Fig. 5*A*). As shown in Fig. 5*B*, melanocytes overexpressing c-MYC showed a noticeable increase in NOXA mRNA, which was further induced (by 4-fold) after treatment with bortezomib. Moreover, melanocytes gained sensitivity to bortezomib in the presence of increased levels of c-MYC (Fig. 5 *C* and *D*). Thus, c-MYC shifted the response of melanocytes from a G_2/M cell cycle arrest to an effective killing, as measured by an increase in sub-G_1 DNA content (Fig. 5*C*), and an enhanced amount of cell death after treatment (Fig. 5*D*).

Functional Impact of c-MYC in Bortezomib-Induced Melanoma Cell Death. Bortezomib is not a rapid death inducer, and at bioavailable doses, it is not sufficient to provide complete responses in mela-

noma (4, 33) and other aggressive cancer types (22). From a therapeutic point of view, it would be important if the occupancy of the NOXA promoter in tumor cells was not saturated (i.e., if increasing the levels of c-MYC could further enhance NOXA expression and, subsequently, cell death). This possibility was evaluated by transducing ectopic c-MYC in representative melanoma cells. Notably, exogenous c-MYC increased the sensitivity to bortezomib by reducing the amount of drug required for the induction of NOXA (Fig. 5*E*). Importantly, ectopic c-MYC favored the response to low doses of bortezomib, increasing caspase processing (Fig. 5*E*), and enhancing by 2-fold the extent of cell death (e.g., compare 85% of viable cells in control-treated populations with 30% when c-MYC is overexpressed) (Fig. 5*F*).

c-MYC was estimated to bind to 10–15% of transcriptionally active genes in the human genome (28), and affect cell viability and apoptosis at multiple levels (34, 35), which may act independently from NOXA. To define the relative contribution of this protein to c-MYC enhanced response to bortezomib, we blocked the endogenous expression of NOXA by a shRNA that we have previously validated (4). Interestingly, this NOXA shRNA reduced the c-MYC-driven killing by bortezomib to the levels of the control parental lines (Fig. 5*G*; $P = 0.009$ in SK-Mel-19 and $P = 0.015$ in SK-Mel-103; see figure legend for statistical analyses). Note that a complete inhibition of cell death was not expected because NOXA is not the sole driver of bortezomib-induced cell death, as previously reported in ref. 4. Therefore, despite the multiple putative targets of c-MYC, the fact that blocking one single gene (NOXA) affects bortezomib-driven killing by c-MYC is highly significant. Together, these results support the potential of enhancing the intrinsic surplus of c-MYC in melanoma cells to activate NOXA, and favor cell death on proteasome inhibition. These data identify a role of c-MYC that may have translational implications for drug design.

Discussion

Complete and sustained proteasome blockage is incompatible with life (36). Even transient inactivation of the proteasome can elicit a variety of changes in gene expression in normal and tumor cells (3). How such a pleiotropic approach can provide a therapeutic index for clinical intervention is poorly understood (2). Here, we identified an unexpected interplay between the proteasome, the proapoptotic protein NOXA, and the oncogene c-*MYC* that provides a molecular explanation for the preferential selectivity of proteasome inhibitors toward tumor cells.

Requirement of c-MYC for the Dual Regulation of NOXA mRNA and Protein by Proteasome Inhibition. Perhaps, one of the most unexpected results from this study is that HIF-1α, E2F-1, or p53, all key proteasomal targets with binding sites at the *NOXA* promoter (12, 15, 16), are largely dispensable in defining the ultimate expression of NOXA protein when the proteasome is blocked. Instead, here, we provide several lines of evidence that support a critical impact of c-MYC on the transcriptional control of *NOXA*. (*i*) By using computational analyses and ChIP methods, we identified and validated three c-MYC binding sites at the *NOXA* promoter. Of those, c-MYC BS III (located at position +84, and within a CpG island) was found to be the most active. (*ii*) Inactivation of this site by mutagenesis abrogated the transcriptional regulation by bortezomib of *NOXA* promoter fragments in luciferase-based reporter assays. (*iii*) Moreover, acetylated histone H3 (classical cofactor of c-MYC) and marker of transcriptionally active chromatin (29–31) was also increased at this c-MYC BS III. The transcriptional regulation of the *NOXA* promoter by c-MYC was further supported by (*iv*) promoter assays with wild-type and mutated c-MYC binding sites and (*v*) the induction of *NOXA* mRNA in cells transduced with ectopic c-MYC. (*vi*) Finally, RNA inference confirmed a key functional role of c-MYC to ultimately allow for the accumulation of this protein on proteasome inhibition.

Our results also emphasize the differential impact of c-MYC on apoptotic modulators of the Bcl-2 family. Thus, c-MYC can induce *NOXA* mRNA, repress the antiapoptotic proteins Bcl-2 or Bcl-x_L (37), activate the proapoptotic factor Bim_{EL} (38), or promote conformational changes in BAX (39). Notably, of all these Bcl-2 family members, only NOXA is regulated in a tumor cell-selective manner (4, 5). The fact that ectopic c-MYC expression can induce the accumulation of NOXA and shift the mode of action of bortezomib from cell cycle arrest to cell death, in otherwise poorly responsive normal melanocytes (Fig. 5 *C* and *D*), provides a molecular explanation for the observation that c-MYC can sensitize primary cells to proteasome inhibition *in vitro* and *in vivo* (40).

The proteasome controls the half-life of the vast majority of cellular proteins (3). Therefore, it would not be expected that bortezomib induced NOXA in malignant cells (even at the mRNA level), solely by stabilizing the endogenous levels of c-MYC. For example, proteasome inhibition can up-regulate various factors (e.g., ERK or JNK) that are frequently hyperactivated in tumor cells, and can modulate c-MYC function (27, 41). Similarly, the transcriptional activity of c-MYC at the *NOXA* promoter can be favored by chromatin remodeling or modification proteins (including histone acetyl transferases), which can be modulated by c-MYC and by the proteasome (41–43). The enrichment of histone H3 acetylation we found at the MYC BS III is consistent with these cooperating events. Still, the critical and preferential role of c-MYC for bortezomib-driven accumulation of NOXA, is illustrated by the dramatic inhibitory effect on NOXA levels on c-MYC shRNA (see model in SI Fig. 11).

Rational Drug Design: Oncogene "Addiction" vs. Oncogene "Surplus." For some tumor cells, a strict dependency or "addiction" to specific oncogenes represents a point of vulnerability that can be exploited for rational drug design (44, 45). This approach has been proven to be highly effective when the targeted oncogene is restricted to tumor cells and controls key events regulating cellular viability. Compounds that block Bcr-Abl, c-*KIT*, Her2, RAF, or EGFR are some examples of genetically targeted therapies with successful clinical activity (45). Interestingly, a variety of experimental models suggest that, at least in certain cancer subtypes, c-MYC may be required for tumor cell maintenance (reviewed in refs. 34 and 46). Based on these results, genetic and pharmacological analyses are being developed to block c-MYC or c-MYC-dependent pathways (see ref. 46 for a recent review). In fact, bortezomib can kill c-MYC depleted melanoma cells in a NOXA-independent manner (M.A.N., M.B.R., and M.S.S, unpublished results).

Blocking c-MYC can compromise the proliferative capacity of normal cells (32, 47). Therefore, instead of targeting c-MYC addiction, exploiting the "surplus" of this oncogene in tumor cells may provide an alternative therapeutic approach. For this strategy to succeed, the molecular circuitry of tumor cells should allow for an efficient, but tumor-restricted, induction of cell death. In the case of bortezomib, here we show that this selectivity can be provided by a preferential activation of NOXA in tumor cells. Importantly, ectopic expression studies suggest that the c-MYC-dependent control of NOXA is not saturated in tumor cells (Fig. 5). Thus, it may be possible to rationally enhance the cytotoxic activity of bortezomib with drugs that further exploit the proapoptotic functions of this oncogene. This may be particularly important in the treatment of aggressive solid tumors, where bortezomib is not sufficient, as a single agent, for the induction of tumor regression.

In summary, this study has identified a mechanism of regulation of NOXA, defined a role of c-MYC in the activation of the apoptotic machinery of tumor cells, and provided a molecular framework that supports the notion of enhancing (instead of blocking) selective oncogenic signals to favor anticancer responses. Together, our results shed information into how a purportedly pleiotropic inactivation of the proteasome can be funneled to discrete oncogenes and their targets. An adroit exploitation of the inherently altered genetic makeup of tumor cells may provide a

powerful strategy to kill malignant cells from "within," while minimizing the risk of unwanted secondary toxicities.

Experimental Procedures

Cells. Normal melanocytes were isolated from neonatal foreskins, as previously described in ref. 4, and maintained in media 254 supplemented with 0.2 mM $CaCl_2$, 16 nM phorbol 12-myristate 13-acetate, and melanocyte growth factors (Cascade Biologics). Melanoma cell lines, MDA-MB-231, and HeLa were cultured in DMEM supplemented with 10% of FBS. Cells were incubated in 7% CO_2, except for the low-oxygen content experiments, where cells were incubated in a hypoxia chamber (Biospherix), supplied with 95% N_2 and 5% CO_2.

Reagents. Bortezomib (Velcade) was obtained from Millennium Pharmaceuticals. DMSO and ActD were from Sigma; and doxorubicin hydrochloride was from Fisher Scientific. The E2F-1 adenovirus has previously been described in ref. 48. shRNAs against c-MYC or NOXA, and siRNAs to block E2F-1 expression are described in *SI Materials and Methods*.

Cell Viability Assays. The percentage of cell death at the indicated times and drug concentrations was estimated by standard trypan blue exclusion or 3-(4,5-dimethylthiazol-2-yl)-2,5-diphenyl tetrazolium bromide (MTT) assays. DNA content was estimated by propidium iodide-based staining and flow cytometry analyses (4). For simplicity, control samples treated only with solvent (0.1–0.05% DMSO) are indicated as NT (nontreated). Processing of apoptotic caspases was analyzed by monitoring the ratio of the full-length inactive proform to processed fragments generated on drug treatment and visualized by Western blotting.

Protein Immunoblots. Total cell lysates were obtained by Laemmli extraction. Protein samples were separated on 12% or 4–20% gradient SDS polyacrylamide gels and transferred to Immobilon-P membranes (Millipore). Protein levels were estimated by densitometry and normalized with respect to Tubulin or β-Actin, used as loading controls. Antibodies used for protein detection are described in *SI Materials and Methods*.

RNA Expression Analyses. The relative expression of NOXA, c-MYC, and CAD mRNA in normal and melanoma cells untreated or treated with bortezomib was determined by RT-PCR using the following primers: *Noxa*, 5′-ATG AAT GCA CCT TCA CAT TCC TCT (forward) and 5′-TCC AGC AGA GCT GGA AGT CGA GTG T (reverse); c-MYC, TCGGATTCTCTGCTCTCCTC (forward) and TCGGTTGTTGCTGATCTGTC (reverse); CAD, AGATGGAAGCGGCCATCAGGAAG (forward) and GGTGGATCTGGAGCATGAGTGG (reverse). Expression levels were normalized to *β-actin* or *GAPDH*.

Promoter Assays. Direct binding of c-MYC to the NOXA promoter by ChIP was addressed by using the EZ-Chip kit from Millipore according to the manufacturer's recommendations. Briefly, 2×10^7 SK-Mel-19 or HeLa cells were fixed in 1% formaldehyde. Chromatin was sheared to an average DNA size of 200–800 bp by sonication using Microson ultrasonic cell disruptor (10 times of 10-s pulses, 50% output). Sonicated chromatin was incubated overnight with 5 μg of anti-c-MYC (N262; Santa Cruz), anti-acetylated Histone H3 (a gift from David Allis) or rabbit IgG (Upstate) antibodies. Immunoprecipitated DNA was de-cross-linked, purified by using columns from the kit and used in a PCR (GC-Rich PCR System; Roche) with the primers listed in *SI Materials and Methods*. PCR products were resolved on 1.5% agarose gel and stained with ethidium bromide. Generation of reporter assays containing wild-type and mutagenized c-MYC binding sites, and characterization of their transcriptional activity are described in *SI Materials and Methods*.

We thank José Esteban, Gabriel Núñez, Keith Wolter, and Colin Duckett for helpful suggestions and critical reading of this manuscript. We also thank Thomas P. Miller for his help with initial analyses of E2F-1 and HIF-1α in melanoma cells, Ryan Stork and Sudha Manava for technical assistance, Andrei Gudkov (Roswell Park Cancer Institute, Buffalo, NY) for the pLV-SV40-Hygro-cMYC, Javier León (University of Cantabria, Santander, Spain) for pGL3-NOXA wild-type-luciferase vector, David C. Allis (The Rockefeller University, New York, NY) for anti-acetyl-histone H3 antibody, and Yi Sun (University of Michigan) for help with hypoxia experiments. This work was supported by Dermatology Foundation Career Development Awards (to M.S.S. and M.A.N.), Elsa U. Pardee Foundation Award (to M.S.S.), and National Institutes of Health Grants R01 CA107237 (to M.S.S.) and CA120244 (to M.A.N.).

1. Richardson PG, Mitsiades C, Hideshima T, Anderson KC (2006) *Annu Rev Med* 57:33–47.
2. Adams J (2004) *Cancer Cell* 5:417–421.
3. Ciechanover A (2005) *Nat Rev Mol Cell Biol* 6:79–87.
4. Fernandez Y, Verhaegen M, Miller TP, Rush JL, Steiner P, Opipari AW, Jr., Lowe SW, Soengas MS (2005) *Cancer Res* 65:6294–6304.
5. Qin JZ, Ziffra J, Stennett L, Bodner B, Bonish BK, Chaturvedi V, Bennett F, Pollock PM, Trent JM, Hendrix MJ, *et al.* (2005) *Cancer Res* 65:6282–6293.
6. Fernandez Y, Miller TP, Denoyelle C, Esteban JA, Tang WH, Bengston AL, Soengas MS (2006) *J Biol Chem* 281:1107–1118.
7. Qin JZ, Xin H, Sitailo LA, Denning MF, Nickoloff BJ (2006) *Cancer Res* 66:9636–9645.
8. Fribley AM, Evenchik B, Zeng Q, Park BK, Guan JY, Zhang H, Hale TJ, Soengas MS, Kaufman RJ, Wang CY (2006) *J Biol Chem* 281:31440–31447.
9. Perez-Galan P, Roue G, Villamor N, Montserrat E, Campo E, Colomer D (2006) *Blood* 107:257–264.
10. Jullig M, Zhang WV, Ferreira A, Stott NS (2006) *Apoptosis* 11:627–641.
11. Hijikata M, Kato N, Sato T, Kagami Y, Shimotohno K (1990) *J Virol* 64:4632–4639.
12. Oda E, Ohki R, Murasawa H, Nemoto J, Shibue T, Yamashita T, Tokino T, Taniguchi T, Tanaka N (2000) *Science* 288:1053–1058.
13. Shibue T, Takeda K, Oda E, Tanaka H, Murasawa H, Takaoka A, Morishita Y, Akira S, Taniguchi T, Tanaka N (2003) *Genes Dev* 17:2233–2238.
14. Villunger A, Michalak EM, Coultas L, Mullauer F, Bock G, Ausserlechner MJ, Adams JM, Strasser A (2003) *Science* 302:1036–1038.
15. Kim JY, Ahn HJ, Ryu JH, Suk K, Park JH (2004) *J Exp Med* 199:113–124.
16. Hershko T, Ginsberg D (2004) *J Biol Chem* 279:8627–8634.
17. Kuwana T, Bouchier-Hayes L, Chipuk JE, Bonzon C, Sullivan BA, Green DR, Newmeyer DD (2005) *Mol Cell* 17:525–535.
18. Chen L, Willis SN, Wei A, Smith BJ, Fletcher JI, Hinds MG, Colman PM, Day CL, Adams JM, Huang DC (2005) *Mol Cell* 17:393–403.
19. Kim H, Rafiuddin-Shah M, Tu HC, Jeffers JR, Zambetti GP, Hsieh JJ, Cheng EH (2006) *Nat Cell Biol* 8:1348–1358.
20. Nijhawan D, Fang M, Traer E, Zhong Q, Gao W, Du F, Wang X (2003) *Genes Dev* 17:1475–1486.
21. Jansson AK, Emterling AM, Arbman G, Sun XF (2003) *Oncogene* 22:4675–4678.
22. Caravita T, de Fabritiis P, Palumbo A, Amadori S, Boccadoro M (2006) *Nat Clin Pract Oncol* 3:374–387.
23. Yu D, Carroll M, Thomas-Tikhonenko A (2007) *Blood* 109:4936–4943.
24. Zeller KI, Zhao X, Lee CW, Chiu KP, Yao F, Yustein JT, Ooi HS, Orlov YL, Shahab A, Yong HC, *et al.* (2006) *Proc Natl Acad Sci USA* 103:17834–17839.
25. Blackwell TK, Huang J, Ma A, Kretzner L, Alt FW, Eisenman RN, Weintraub H (1993) *Mol Cell Biol* 13:5216–5224.
26. Kim JW, Zeller KI, Wang Y, Jegga AG, Aronow BJ, O'Donnell KA, Dang CV (2004) *Mol Cell Biol* 24:5923–5936.
27. Hann SR (2006) *Semin Cancer Biol* 16:288–302.
28. Adhikary S, Eilers M (2005) *Nat Rev Mol Cell Biol* 6:635–645.
29. Clayton AL, Hazzalin CA, Mahadevan LC (2006) *Mol Cell* 23:289–296.
30. Fischle W, Wang Y, Allis CD (2003) *Curr Opin Cell Biol* 15:172–183.
31. Cowling VH, Cole MD (2006) *Semin Cancer Biol* 16:242–252.
32. Wang H, Mannava S, Grachtchouk V, Zhuang D, Soengas MS, Gudkov AV, Prochownik EV, Nikiforov MA, *Oncogene*, 10.1038/sj.onc.1210823.
33. Amiri KI, Horton LW, LaFleur BJ, Sosman JA, Richmond A (2004) *Cancer Res* 64:4912–4918.
34. Meyer N, Kim SS, Penn LZ (2006) *Semin Cancer Biol* 16:275–287.
35. Kim JW, Gao P, Liu YC, Semenza GL, Dang CV (2007) *Mol Cell Biol* 27:7381–7393.
36. Ciechanover A (1998) *EMBO J* 17:7151–7160.
37. Eischen CM, Woo D, Roussel MF, Cleveland JL (2001) *Mol Cell Biol* 21:5063–5070.
38. Hemann MT, Bric A, Teruya-Feldstein J, Herbst A, Nilsson JA, Cordon-Cardo C, Cleveland JL, Tansey WP, Lowe SW (2005) *Nature* 436:807–811.
39. Juin P, Hunt A, Littlewood T, Griffiths B, Swigart LB, Korsmeyer S, Evan G (2002) *Mol Cell Biol* 22:6158–6169.
40. Orlowski RZ, Eswara JR, Lafond-Walker A, Grever MR, Orlowski M, Dang CV (1998) *Cancer Res* 58:4342–4348.
41. Dang CV, O'Donnell KA, Zeller KI, Nguyen T, Osthus RC, Li F (2006) *Semin Cancer Biol* 16:253–264.
42. Guccione E, Martinato F, Finocchiaro G, Luzi L, Tizzoni L, Dall' Olio V, Zardo G, Nervi C, Bernard L, Amati B (2006) *Nat Cell Biol* 8:764–770.
43. Knoepfler PS, Zhang XY, Cheng PF, Gafken PR, McMahon SB, Eisenman RN (2006) *EMBO J* 25:2723–2734.
44. Sharma SV, Gajowniczek P, Way IP, Lee DY, Jiang J, Yuza Y, Classon M, Haber DA, Settleman J (2006) *Cancer Cell* 10:425–435.
45. Weinstein IB, Joe AK (2006) *Nat Clin Pract Oncol* 3:448–457.
46. Vita M, Henriksson M (2006) *Semin Cancer Biol* 16:318–330.
47. de Alboran IM, O'Hagan RC, Gartner F, Malynn B, Davidson L, Rickert R, Rajewsky K, DePinho RA, Alt FW (2001) *Immunity* 14:45–55.
48. Nahle Z, Polakoff J, McCurrach ME, Davuluri RV, Narita M, Jacobson MD, Zhang MQ, Lazebnik Y, Bar-Sagi D, Lowe SW (2002) *Nat Cell Biol* 4:859–864.